Non-Cartesian POCSENSE

A. Samsonov[1], C. Johnson[1]

[1]Scientific Computing and Imaging Institute, University of Utah, Salt Lake City, Utah, United States

Introduction: Projections onto convex set (POCS) formalism presents a powerful mathematical apparatus for solving many reconstruction problems that entail incomplete and inconsistent data. Recently, POCS formalism has been adopted for reconstruction of sensitivity encoded MRI data in fast and efficient iterative POCSENSE procedure [1, 2]. POCSENSE allows simple and computationally efficient inclusion of many nonlinear constraints (i.e., phase constraint [3]) in image reconstruction to improve image quality or to achieve high degrees of data acquisition speedup. However, the application of the original POCSENSE was previously limited to the Cartesian *k*-space sampling. In this work, we propose extension of POCSENSE technique that is able to handle data sampled on arbitrary trajectories.

Theory: The iteration of POCSENSE technique includes several projections onto data and additional convex sets (see Algorithm). Here, s_i – coil sensitivities, i=1…N_C, and * denotes complex conjugation. Projection onto data set is accomplished by resetting the *k*-space samples at the trajectory positions to the original values. The reconstruction is accomplished on a Cartesian grid to make use of the fast Fourier transform algorithm (FFT). Hence, the projection is straightforward, if the original trajectory coincides with the Cartesian grid points. However, in POCS algorithms, which deal with data sampled at arbitrary positions, this projection operation gets more complicated [4]. Let $\boldsymbol{r}$ and $\boldsymbol{k}$ denote image space and *k*-space coordinates respectively, $\boldsymbol{K}$ - the set of sampled positions, $m_{i,0}(\boldsymbol{k})$ – data acquired by the *i*-th coil at $\boldsymbol{k}\in\boldsymbol{K}$, $m_{i,c}(\boldsymbol{k})$ - *k*-space values for the *i*-th coil image on the current iteration, i=1, …N_C. Then, the data projection step for the *i*-th coil to be used with arbitrary trajectories is defined as follows:

Algorithm. POCSENSE (non-accelerated version).

Step 1: $g_i^{(n+1)} = P_i^{data}(s_i f^{(n)}),\ i = 1,\ldots N_C$ *(Project in parallel onto data convex sets)*

Step 2: $t^{(n+1)} = \left(\sum_{i=1}^{N_C} g_i^{(n+1)} s_i^*\right) \Big/ \left(\sum_{i=1}^{N_C} |s_i|^2\right)$ *(Combine the projection results)*

Step 3: $f^{(n+1)} = P_A(t^{(n+1)})$ *(Project onto additional convex sets)*

$$g_i^{(n+1)} = P_i^{data}(s_i f^{(n)}) \Leftrightarrow a)\ m_{i,c}^{(n)} = F(s_i f^{(n)});\ b)\ m_{i,c}^{(n+1)} = m_{i,c}^{(n)} + G_{AC}(m_{i,0} - G_{CA} m_{i,c}^{(n)});\ c)\ g_i^{(n+1)} = F^{-1}(m_{i,c}^{(n+1)}) \qquad (1)$$

Here, G_{AC} and G_{CA} are interpolation operations transferring the data from the original trajectory to a Cartesian grid and vice versa, and F and F^{-1} are forward and inverse FFTs respectively. In order to update the *k*-space values, the current Cartesian *k*-space estimate is first regridded to the original trajectory. Then, the difference between acquired and updated values is taken to produce a set of error measurements. Finally, the error is transferred back to Cartesian grid and used to correct the *k*-space values.

Methods: We utilized standard gridding with a Kernel-Bessel kernel [5] to implement interpolation operations, and Pipe's method [6] to find sampling density compensation function. Our implementation of Eq. (1) is depicted in Fig. 1. The parameters of the kernel were chosen as L=3, B=14.1372, and the overgridding parameter was taken equal to 2. The phantom data were obtained using a standard GE spiral scan (18 interleaves, 2048 points per interleave, image matrix 192-by-192) on 1.5T GE SIGNA MR scanner (GE Medical Systems, Milwaukee, WI), equipped with a custom-built four-element (N_c=4) bilateral temporal lobe phased array coil. The reduced dataset was produced taking every second interleave of the full dataset. The sensitivity maps were estimated by smoothing the reference images obtained from the full dataset and normalized by sum-of-squares image.

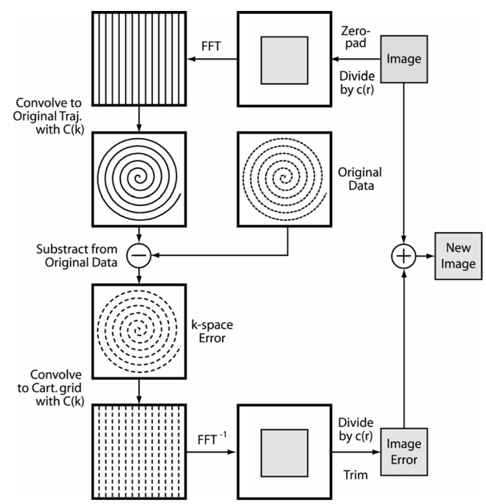

Figure 1. Implementation of data projection operator using gridding interpolation. Here, C($\boldsymbol{k}$) is *k*-space convolution kernel, c($\boldsymbol{r}$) – its image space counterpart. Sampling density compensation is accomplished before each convolution operation.

Results: Figure 2 shows results of reconstruction of spiral data from phantom scan. The image reconstructed from the original data contains significant aliasing artifacts (Fig. 2a). In the image reconstructed by non-Cartesian POCSENSE, the artifacts are eliminated to a negligible level (Fig. 2b). For comparison, the reference image was produced by regridding the full spiral dataset (Fig. 2c).

Discussion: We developed a new POCSENSE technique that could handle sensitivity encoded data sampled on arbitrary trajectories. The new technique makes available benefits of POCS formalism to a wide range of *k*-space acquisition approaches. The new algorithm is computationally and memory efficient compared to the reconstruction methods based on the direct matrix inversion. For many trajectories such as radial, the *k*-space center is often oversampled. In this case, it is possible to accurately interpolate all Cartesian grid points in the area. Then, hybrid approach may be employed that combines traditional data projection for *k*-space center and the new method for the outer, undersampled regions. This promises to significantly decrease the complexity associated with gridding part of the method. The implementation of POCS iteration described here could be used in other POCS-based reconstructions of non-Cartesian data, i.e. partial *k*-space reconstruction for variable-density spirals [7].

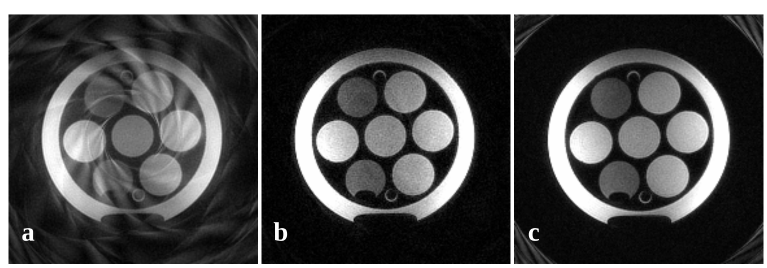

Figure 2. Reconstruction of spiral data using non-Cartesian POCSENSE. Undersampled image (a) was obtained from full spiral dataset (c) by taking every second interleave. Image after 9 iterations of non-Cartesian POCSENSE is shown in (b). The reconstructed image is characterized by minimized residual aliasing artifact and improved resolution. At the same time, the noise level is higher then in the full image (c) that is common for any method of reconstruction of reduced datasets.

Acknowledgments: This work was supported by NIH BISTI grant 1P20HL68566-01.

References:

[1] Kholmovski EG, et al, Proc ISMRM 2002, p. 194
[2] Samsonov AA, et al, Proc ISMRM 2003; p. 2343
[3] Samsonov AA, et al, Proc ISMRM 2002; p. 2408
[4] Sauer KD, et al, IEEE CAS-34, 1987;12:1497-1506
[5] Jackson JI, et al, IEEE TMI 1991;MI-10:473-478
[6] Pipe JG, et al, MRM 1999;41:179-186
[7] Lee J, et al, Proc ISMRM 2003, p 475